## PAPER

Check for updates

# Development of the telescoped flow Pd-catalyzed aerobic alcohol oxidation/reductive amination sequence in the synthesis of new phosphatidylinositide 3-kinase inhibitor (CPL302415)†

Stanisław Michałek, [ID] * Anna M. Maj, [ID] * Lidia Gurba-Bryśkiewicz, [ID]
Wioleta Maruszak, [ID] Krzysztof Wiśniewski, Marcin Zagozda, Mariola Stypik,
Krzysztof Dubiel and Maciej Wieczorek

Herein, we describe a two-step sequential flow synthesis: Pd-catalyzed aerobic oxidation to an aldehyde **2**, which is then converted by reductive amination in H-Cube® PRO into CPL302415 (**3**). CPL302415 is our new PI3Kδ inhibitor, which is now under evaluation for the treatment of systemic lupus erythematosus. The process was optimized using the DoE approach and generalized to other biologically active derivatives of CPL302415.

Due to advantages such as high efficiency, safety and precise reaction control, continuous flow technology has become an attractive alternative to the batch process, including the synthesis of active pharmaceutical ingredients (APIs).[1] Moreover, reactions carried out in flow enable the combination of multiple transformations into one procedure, the so-called telescoped synthesis,[2] thereby avoiding manual workup between different stages and reducing solvent consumption. This consequently leads to a reduction in the amount of solvent-related waste, which is usually a determining factor in environmental impact. For example, GlaxoSmithKline (GSK) reported that solvent-related waste represents 80% of all waste.[3] The additional advantage of the flow process is the use of small-diameter tubes, which allows for better mass/heat transfer and more effective mixing, and consequently, lower energy consumption. Therefore, although developing a flow method is a very labor-intensive task and initially more difficult to implement than batch synthesis, continuous API production is considered not only more sustainable[4] but also more economical and is therefore supported by regulatory agencies.[5] Recently, our laboratory became interested in transforming selected batch reactions into flow procedures.[6] One of these was the synthesis of CPL302415 (Fig. 1), a new promising PI3Kδ inhibitor and a member of the first class PI3K (phosphoinositide 3-kinase) inhibitors.[7] This type of compound regulates the differentiation, proliferation, migration, and survival of

immune cells, enabling therapeutic opportunities for the treatment of inflammatory and autoimmune diseases, including asthma and systemic lupus erythematosus (SLE).[8] CPL302415 is now under evaluation for the treatment of systemic lupus erythematosus.

The aim of this work was to develop a new, simple, high-yielding, flow-through, lab-scale method for the reductive amination of 5-[2-(difluoromethyl)-1*H*-benzimidazol-1-yl]-7-(morpholin-4-yl)pyrazolo[1,5-*a*]pyrimidine-2-carbaldehyde (**2**) to 1-{2-[(4-*tert*-butylpiperazin-1-yl)methyl]-7-(morpholin-4-yl)pyrazolo[1,5-*a*]pyrimidin-5-yl}-2-(difluoromethyl)-1*H*-benzimidazole (**3**) and combine it in a telescoped sequence with the antecedent precursor in the synthesis pathway, flow oxidation of {5-[2-(difluoromethyl)-2,3-dihydro-1*H*-1,3-benzodiazol-1-yl]-7-(morpholin-4-yl)pyrazolo[1,5-*a*]pyrimidin-2-yl}methanol (**1b**) (Fig. 1). The third objective was to generalize the established
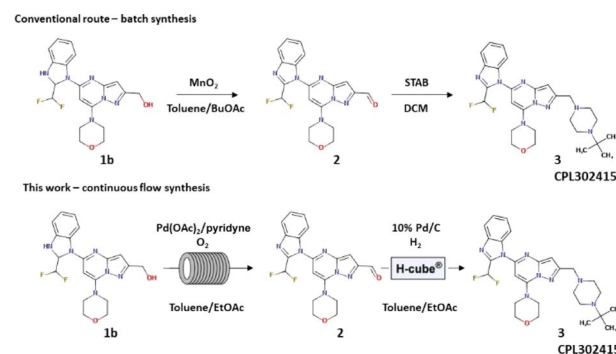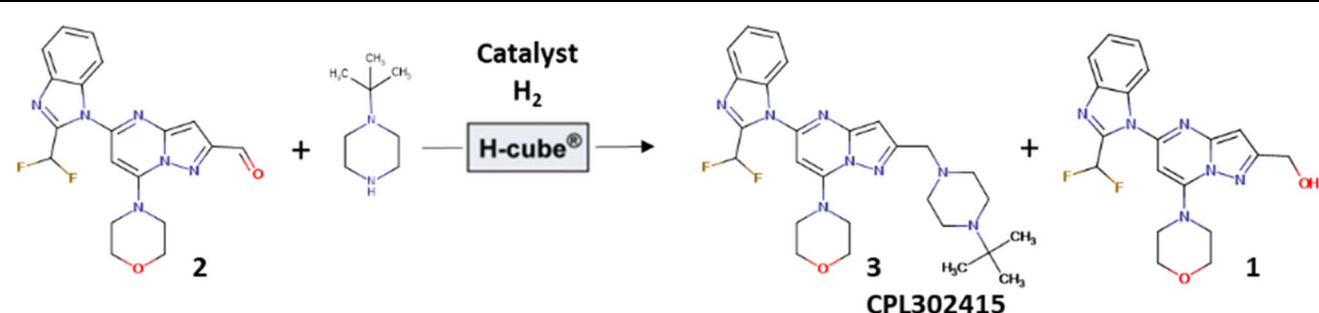
*Celon Pharma S.A., ul. Marymoncka 15, 05-152 Kazuń Nowy, Poland. E-mail: stanislaw.michalek@celonpharma.com; anna.maj@celonpharma.com*

† Electronic supplementary information (ESI) available. See DOI: https://doi.org/10.1039/d4ra04923c



Fig. 1 The two final steps in the synthesis pathway of CPL302415.

**Table 1** Screening of the catalyst and solvent for the reductive amination of **2** carried out under flow conditions[a]



CPL302415

| Entry | Catalyst | Solvent | Eq. of N-tert-butylpiperazine | $T$ (°C) | $P_{sys}$ (bar) | Flow of reagent (mL min$^{-1}$) | Flow of H$_2$ (mL min$^{-1}$) | % of **2**[b] | % of **1**[b] | % of **3**[b] |
|---|---|---|---|---|---|---|---|---|---|---|
| 1 | 20% Pd(OH)$_2$/C | MeOH | 4 | 50 | 3 | 1 | 60 | 92.5 | 1.2 | 4.6 |
| 2 | | | | 70 | 3 | 1 | 6 | 11.0 | 22.3 | 57.2 |
| 3 | | | | 70 | 1 | 1 | 6 | 46.5 | 1.9 | 46.7 |
| 4 | | DCM | 1.2 | 70 | 10 | 0.5 | 6 | 54.7 | 9.7 | 28.3 |
| 5 | | | 4 | 50 | 1 | 1 | 6 | 0.1 | 99.4 | 0.2 |
| 6 | | DMA | 4 | 70 | 3 | 0.5 | 6 | 0 | 98.7 | 0.3 |
| 7 | | Dioxane | 4 | 70 | 3 | 1 | 6 | 20.8 | 10.7 | 65.8 |
| 8 | | | 4 | 90 | 3 | 0.5 | 6 | 0 | 13.7 | 81.8 |
| 9 | | Toluene/EtOAc (1/1) | 2 | 90 | 3 | 0.3 | 18 | 0 | 10.7 | 43.5 |
| 10 | 10% Pd/C | Toluene/EtOAc (1/1) | 2 | 90 | 3 | 0.3 | 18 | 0 | 8.9 | 87.7 |

[a] Standard reaction conditions: substrate = 220 mg (0.552 mmol) and 157 mg N-tert-butylpiperazine were dissolved in selected solvent (8 mL); CatCart® 70 mm long, containing 20% Pd(OH)$_2$/C 380 ± 5 mg and 10% Pd/C 260 ± 5 mg. [b] % determined by UHPLC; for details see ESI.

protocol in order to quickly build a chemical library of other biologically active potential PI3Kδ inhibitors based on the pyrazolo[1,5-a]pyrimidine core. Additionally, we aimed to make the whole synthesis environmentally sustainable and easy to integrate at a large scale for the potential production of active pharmaceutical ingredients (API) (CPL302415).

In one of our previous articles, we thoroughly described the development and optimization of the very effective and selective Pd-catalyzed flow aerobic oxidation of alcohol **1b** to aldehyde **2**;[6a] thus, we were primarily interested in developing the reductive amination of 5-[2-(difluoromethyl)-1H-benzimidazol-1-yl]-7-(morpholin-4-yl)pyrazolo[1,5-a]pyrimidine-2-carbaldehyde (**2**). Typically, reductive amination is carried out with stoichiometric reductors such as sodium cyanoborohydride (NaBH$_3$CN)[9] or sodium triacetoxyborohydride [NaBH(OAc)$_3$].[10] However, due to better atom economy, more convenient processing as well as lower quantity of waste formed during the reaction, its catalytic version was more extensively studied and also used in industrial application. The significant examples of such processes were published by Genzyme Corporation,[11] Janssen Research & Development[12] or Eli Lilly and Company.[13] Thus, we preferentially chose to perform this transformation with H$_2$ as a reductor and with a fixed-bed catalyst in order to avoid catalyst separation from the reaction mixture, which is very convenient in the late stage of API synthesis. The experiments were performed using the continuous-high pressure hydrogenation apparatus, H-Cube® Pro from ThalesNano, where hydrogen was generated by the

electrolysis of water and mixture of dissolved reagents and gas was pumped through a suitable fixed-bed catalyst encapsulated in a metal cartridge. The preliminary tests results are gathered in Table 1. The reactions were realized in the presence of 20% Pd(OH)$_2$/C and 10% Pd/C both with CatCart® 70 mm length, containing 380 ± 5 mg and 260 ± 5 mg of the catalyst, respectively. The reactions were carried out in MeOH, DCM, DMA, dioxane, and toluene/EtOAc (1/1) mixture, and the temperature was varied from 50 °C to 90 °C. The best yield (87.7%) of the desired product **3** was observed in the presence of toluene/EtOAc (1/1) mixture at 90 °C under 3 bar of system pressure with flow of H$_2$ = 18 mL min$^{-1}$ and flow of reagents = 0.3 mL min$^{-1}$. Moreover, the results show that 10% Pd/C is twice as effective as 20% Pd(OH)$_2$/C (Table 1; entries 9 and 10); under the same conditions, we obtained 43.5% of **3** with 20% Pd(OH)$_2$/C and 87.7% with 10% Pd/C. Taking into account that 10% Pd/C CatCart® is 40% chipper than 20% Pd(OH)$_2$/C and that the previously described flow aerobic oxidation of primary alcohol **1b** to aldehyde **2** was carried out in toluene/EtOAc 1 : 1 mixture, as well as our main objective, which is the development of the telescoped sequence, we were interested in keeping a mixture of toluene/EtOAc as a convenient choice of solvent and 10% Pd/C as the catalyst in the reductive amination. To select the most appropriate reaction conditions, we applied the design of experiment (DoE) approach.[14] The DoE study and statistical analysis were performed using the design of experiment tools of STATISTICA software (v.13.3). We implemented central composite design (CCD) and response surface methodology

(RSM) $2^{(5)}$, including two repetitions at a central point for the reproducibility study. The following parameters were considered for the multivariate optimization, *i.e.*, temperature (in the range of 70–100 °C), system pressure (between 1 and 5 bar), flow of reagents (between 0.3 and 2.1 mL min$^{-1}$), flow of H$_2$ (between 6 and 48 mL min$^{-1}$), and the equivalent of *N-tert*-butylpiperazine (between 1.2 and 4.0) (Table S1†). The fit of the obtained RSM model was $R^2 = 0.69$ (Fig. S1†). ANOVA analysis shows that the main statistically significant effect on the yield of product **3** is the interaction effect between the equivalent of *N-tert*-butylpiperazine and the temperature ($p = 0.0037$), which has a negative influence. The second very important statistically effect is the linear positive influence of *N-tert*-butylpiperazine equivalents ($p = 0.0110$). Next, we also observed the linear negative effect of the reagents flow ($p = 0.0221$), negative interaction effect of temperature and system pressure ($p = 0.0262$), negative interaction effect between the temperature and H$_2$ flow ($p = 0.0276$), positive interaction effect of reagents flow and hydrogen flow ($p = 0.0313$), and at the end, negative quadratic effect of temperature ($p = 0.0487$) (Fig. S1†). From the results of the RSM model, the maximum predicted CPL302415 product **3** yields were in the temperature range from 70 °C to 90 °C, system pressure range from 1.6 to 4.2 bar, flow of reagents range from 0.3 to 0.7 mL min$^{-1}$, flow of H$_2$ range from 6 to 32 mL min$^{-1}$, and equivalent of *N-tert*-butylpiperazine range from 3.4 to 4.0 (Fig. S1†). In the next step, we experimentally investigated the influence of the reaction temperature on the yield of the desired product **3** (CPL302415) in the chosen toluene/EtOAc mixture in the presence of the most effective conditions in the preliminary screening of the 10% Pd/C catalyst. In this series of experiments, the temperature was varied in the range of 70–110 °C, the flow of the hydrogen was fixed at 18 mL min$^{-1}$, the rate of reagents flow was 0.7 mL min$^{-1}$, and the system pressure was maintained at three bar; the last three parameters were established based on the range obtained in DoE analysis. In order to improve the economic aspect of the reaction and keeping in mind the green metrics as well as the limited solubility of reagents during flow oxidation, we tried to

decrease the equivalents of *N-tert*-butylpiperazine compared to the optimum obtained from the DoE model and we kept two equivalents of *N-tert*-butylpiperazine. The results shown in the graph (Fig. 2) show that the highest yield of the product **3** (93%) was observed at 90 °C; a further increase in temperature resulted in a decrease in the quantity of product **3** to 87% at 110 °C. We also noticed that at 90 °C, increasing the hydrogen flow from 18 mL min$^{-1}$ to 30 mL min$^{-1}$ resulted in a significant decrease in the amount of **3** from 93% to 86.2%.

Next, we were also interested in the stability and performance of the ThalesNano CatCart® 10% Pd/C 70 mm cartridge in the reductive amination of our substrate 5-[2-(difluoromethyl)-1*H*-benzimidazol-1-yl]-7-(morpholin-4-yl)pyrazolo[1,5-*a*]pyrimidine-2-carbaldehyde (**2**). Thus, for this purpose, 148 mL of the solution containing 8.38 g of aldehyde **2** was pumped through the catalyst cartridge (10% Pd/C; 70 mm long) under the optimized conditions for 6 h 15 min and samples were taken regularly (Fig. 3). Even after this time, we obtained 93–94% of **3**; the results demonstrate very high performance of the 10% Pd/C catalyst in the transformation, and no adsorption of product **3** on the catalyst cartridge was observed. Furthermore, the ICPMS of the crude reaction mixture from this experiment detected only 0.005 ppm of Pd.

In the next series of experiments, we additionally compared three catalysts, namely, 5% Pd/C; 10% Pd/C and 20% Pd(OH)$_2$/C, sealed in a commercially available CatCart® 30 mm (Fig. 4A). In this case, the reaction was carried out at 90 °C under 3 bar of system pressure with the hydrogen rate fixed at 18 mL min$^{-1}$ and the flow of reagents at 0.3 mL min$^{-1}$. The highest quantity of **3** (79.1%) was obtained for 10% Pd/C. We also observed that using CatCart® 30 mm, the optimum flow of hydrogen was 30 mL min$^{-1}$. Increasing the H$_2$ flow rate from 18 mL min$^{-1}$ to 30 mL min$^{-1}$ let us boost the amount of **3** to 82.6%, further increasing of the hydrogen flow, which resulted in a lower percent of **3** with 42 mL min$^{-1}$, which was 79.8% (Fig. 4B).

With the two last optimized steps of CPL302415 synthesis, we started to combine the reactions into one telescoped continuous flow sequence, where we used toluene/EtOAc mixture and Pd-based catalysts in both transformations. Fig. 5
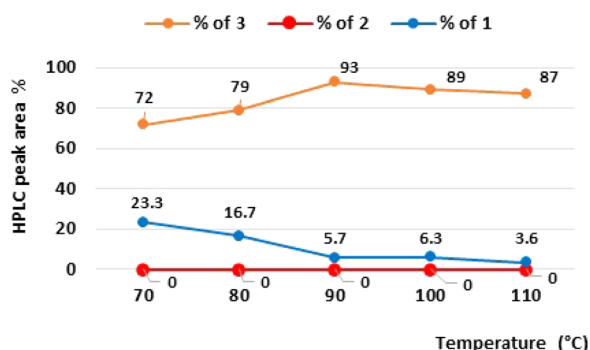


**Fig. 2** Reductive amination of **2** towards product **3**—temperature influence. Conditions: 0.01 M solution of **2** + 2 equiv. of *N-tert*-butylpiperazine in toluene/EtOAc mixture; H-Cube® Pro: 10% Pd/C 70 mm, $P_{sys}$ = 3 bar, flow of reagents = 0.7 mL min$^{-1}$; flow of H$_2$ = 18 mL min$^{-1}$. Conversion of **2** and selectivity for **1** and **3** were determined by UHPLC.
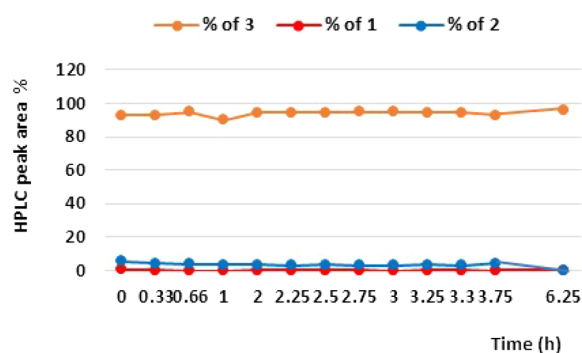


**Fig. 3** Stability of the catalyst. Conditions: 0.01 M solution of **2** + 2 equiv. of *N-tert*-butylpiperazine; H-Cube® Pro: 10% Pd/C 70 mm, 90 °C, $P_{sys}$ = 3 bar, flow of reagents = 0.7 mL min$^{-1}$; flow of H$_2$ = 18 mL min$^{-1}$. Conversion of **2** and selectivity for **3** and **1** were determined by UHPLC.
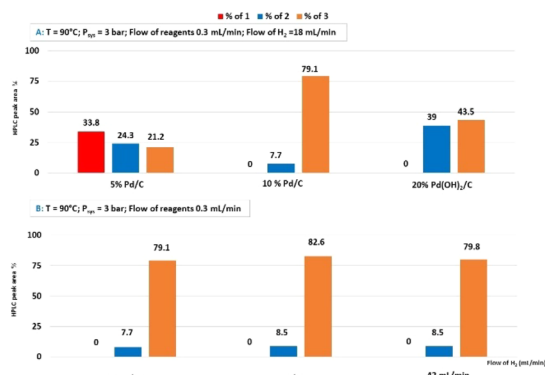
**Fig. 4** (A) Performance of different CatCart® length 30 mm in the reductive amination of **2** towards product **3** in toluene/EtOAc (1 : 1). (B) Reductive amination of **2** towards product **3**—influence of hydrogen rate; 10% Pd/C CatCart® length 30 mm. Conversion of **2** and selectivity for **1** and **3** were determined by UHPLC.

represents our approach to the telescoped protocol for the synthesis of CPL302415 (for detailed description of applied equipment, see ESI†). The first test of the telescoped sequence protocol was carried out applying the optimized procedures that were established independently for each step. The aerobic oxidation of alcohol was performed according to the described procedure[6a] using two combined Vapourtec easy-Medchem systems together with four PFA tubular reactors (10 mL, id = 1 mm). The two liquid feeds were introduced with peristaltic pumps and oxygen gas was introduced through a mass flow controller (Vapourtec SF-10 pump; input pressure 5 bar). The system solvent bottle was filled with toluene/EtOAc (1/1) mixture. The substrate feed and gas feed were mixed using a Y-shaped mixer, then run through a 28 cm (id = 1 mm) tube to enable the substrate solution to saturate it with oxygen and later combined with the catalyst solution. This part of the experiment was controlled with FlowWizard™ software, which calculated

the reaction time and operated the easy-Medchem system. The oxidation step was carried out with 20 mol% of Pd(OAc)$_2$/pyridine = 1/1.3 at $T = 120$ °C under $P_{O_2} = 5$ bar and with $V_{O_2} = 0.1$ mL min$^{-1}$; $V_{reagents} = 1$ mL min$^{-1}$, which resulted in 84% yield of **2**. Next, the reaction mixture was pumped through the filter with neutral aluminum oxide, and after that, the third stream with a solution of *N-tert*-butylpiperazine in toluene/EtOAc (1/1) mixture was added, keeping the **2**/*N-tert*-butylpiperazine ratio constant at 1 eq./2 eq. Then, the mixture was passed through two combined PFA tubular reactors (20 mL, id = 1 mm) and one PFA tubular reactor (10 mL, id = 1 mm) at 50 °C in order to generate the imine. On account of the fact that oxidation takes place using pure oxygen at a pressure of 5 bar and the subsequent reductive amination involves molecular hydrogen, for safety reasons, we decide to interrupt our single-flow system and introduce an additional container into the line. In order to remove oxygen from the reaction mixture, the tank was placed in an ultrasonic bath and the solution was additionally rinsed with argon. The second reason why we decided to disrupt the flow is the difference in the flow rate of the reactants between the two stages. In oxidation, the total speed of reactants is 2.1 mL min$^{-1}$, while in reductive amination, the initial reagent speed is 0.7 mL min$^{-1}$. The interruption in the flow process also let us take the sample after the first stage. In the final step, the reaction mixture is pumped from the tank by the H-Cube® Pro apparatus, where it is mixed with H$_2$ and passed through 10% Pd/C, CatCart® 70 mm length. The reaction was controlled by H-Cube® Pro ThalesNano software. During the amination reductive, we kept the temperature at 90 °C, flow of the hydrogen was fixed on 18 mL min$^{-1}$, the rate of reagents flow was 0.7 mL min$^{-1}$, and the system pressure was maintained at 3 bar. In this experiment, which was conducted twice, we observed product **3** yields of 72 and 74%. Thus, we consider that this process is quite reproductive and we can also add that the small quantities of Pd(OAc)$_2$/pyridine, which still may be present in the reactant solution, did not poison the 10% Pd/C
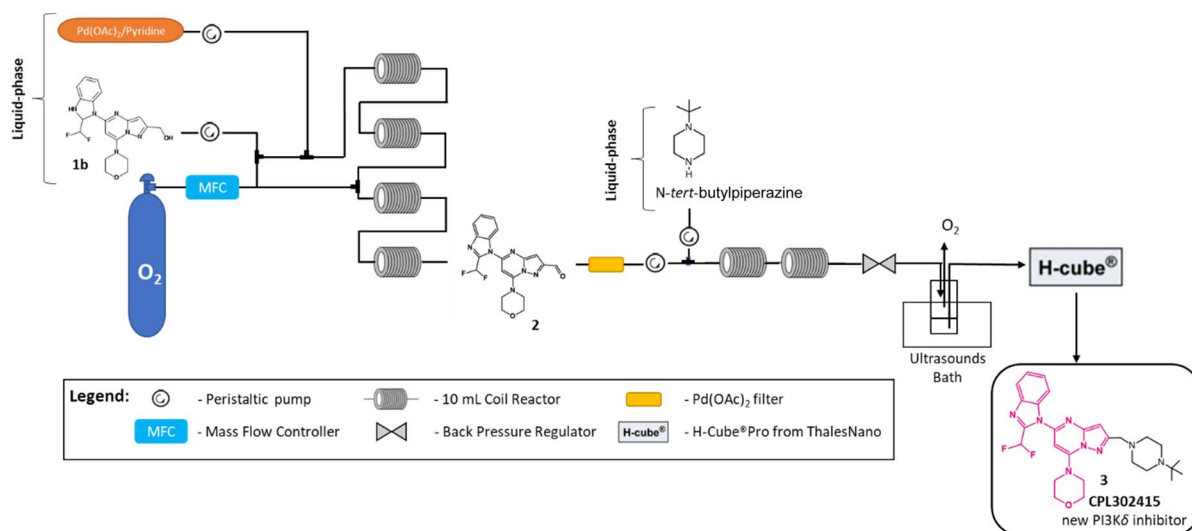


**Fig. 5** Telescoped flow Pd–catalyzed aerobic alcohol oxidation/reductive amination of alcohol **1b** to CPL302415 (**3**).

catalyst. The whole process was analyzed after each step by off-line UHPLC.

The first screening and optimization of reductive amination was performed at a higher concentration than that achievable after flow oxidation. Thus, to better match the two steps of our flow process, we carried out the additional small tuning of all protocols applying DoE design. The DoE study and statistical analysis were performed using the design of experiment tools of STATISTICA software (v.13.3). In one of our previous articles, we fully described the optimization of the oxidation step[6a] and we already know that in this transformation, we have no margin for further increasing the efficacy and process intensity. For all these reasons, we decided to optimize only the speed of the reagents in reductive amination in the range of 0.7–1.2 mL min$^{-1}$ and the hydrogen flow rate in the range of 6–30 mL min$^{-1}$. The raw results are shown in Table 2.

Statistical analysis of the prediction model shows that the flow of H$_2$ has the greatest influence on the yield of product **3** and is a negative effect. On the other hand, the interaction between the flow of hydrogen and the flow of the reagents is slightly positive for the yield of product **3** (Fig. S2†). The response surface fitted to the calculated model is shown in Fig. 6.

The optimal range of input parameters to obtain the maximum yield of the product (**3**) was from 6 mL min$^{-1}$ to 11.5 mL min$^{-1}$ of the hydrogen flow rate for the reagents flow rate of 0.7 mL min$^{-1}$ (the red area in Fig. 6). The ICPMS analysis of the crude reaction mixture from the telescoped sequence experiment detected 38.847 ppm of Pd.

We also explored the generalizability of this procedure for the synthesis of other PI3Kδ inhibitors based on the pyrazolo[1,5-a]pyrimidine core and by reductive amination (**2**) with various piperazine derivatives such as (cyclopropylcarbonyl)piperazine, 2-(4-piperidyl)-2-propanol or 2-methyl-2-2(piperazin-1-yl)propanamide (Table 3). The reactions were carried out in the presence of 10% Pd/C CatCart® 70 mm under the conditions optimized for N-tert-butylpiperazine, i.e., 2
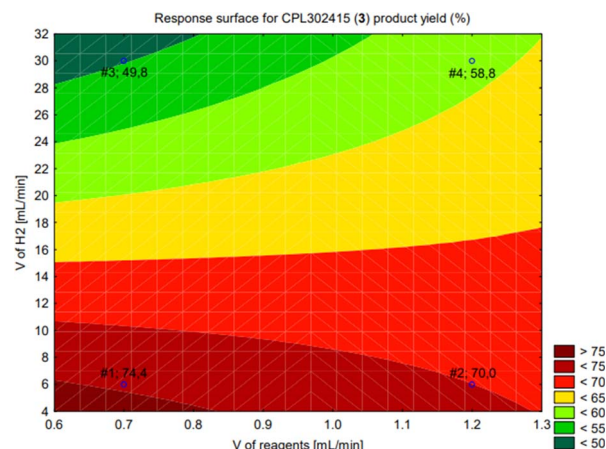


**Fig. 6** Response surface for the yield of CPL302415 (**3**) (%) at $P_{sys}$ = 3 bar; $T$ = 90 °C; 2 equivalents of N-tert-butylpiperazine.

equivalents of piperazine derivative, 90 °C, the hydrogen flow was set at 18 mL min$^{-1}$, the reagent rate was 0.7 mL min$^{-1}$ and the system pressure was maintained at 3 bar. For all the tested piperazine derivatives, complete aldehyde conversion and high yield of the desired product from 85 to 88% were observed.

Moreover, we investigated the sustainability of batch and flow processes by calculating selected green metrics for both the methods.[15] The first graph in Fig. 7a shows the radial polygon performance of reductive amination for batch and flow processes compared to the ideal green values. Fig. 7b represents the performance of the last two steps combined together in the synthesis of CPL302415, i.e., oxidation and reductive amination, carried out in batch syntheses as well as by telescoped flow sequence. Considering only the reductive amination step, almost all of the examined parameters, i.e., atom economy (AE), reaction yield (rxn yield), material recovery parameter (MRE), and reaction mass efficiency (RME), were more favorable and closer to the ideal values for the flow process (Fig. 7a; Table 4; for calculations details, see ESI†). Similarly, calculations

**Table 2** Input parameters and results from DoE full design $2^2$ performed in telescoped flow Pd-catalyzed aerobic alcohol oxidation/reductive amination of alcohol **1b** to CPL302415 (**3**) – optimization of the reductive amination[a]



| Entry | V of reagents (mL min$^{-1}$) | V of H$_2$ (mL min$^{-1}$) | Conv. of **1b**[b] (%) | % of **2**[b] | % of **1b**[b] | % of **1b**[b] | % of **3**[b] |
|---|---|---|---|---|---|---|---|
| 1 | 0.7 | 6 | 78.6 | 0.0 | 21.4 | 0.7 | 74.5 |
| 2 | 1.2 | 6 | 76.9 | 0.2 | 23.1 | 2.3 | 70.0 |
| 3 | 0.7 | 30 | 68.7 | 0.3 | 31.3 | 11.9 | 49.8 |
| 4 | 1.2 | 30 | 68.9 | 0.2 | 31.1 | 5.1 | 58.8 |

[a] Standard reaction conditions: substrate **1b** = 20 mg (0.05 mmol) dissolved in 2 mL toluene/EtOAc = 1 : 1, $P_{sys}$ = 3 bar; $T$ = 90 °C; 2 equivalents of N-tert-butylpiperazine. [b] Determined by UHPLC; for details, see ESI.
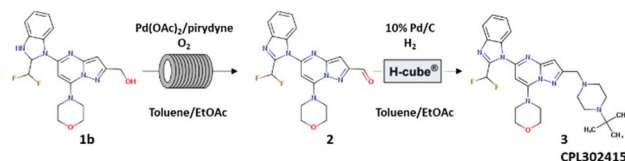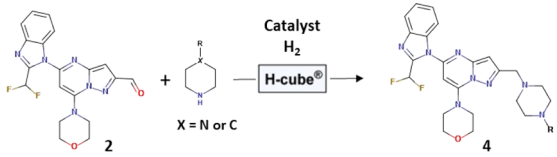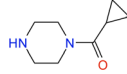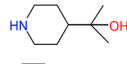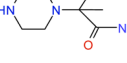
**Table 3** Reductive amination of **2** in the presence of different piperazine derivatives carried out under flow conditions[a]



| Entry[a] | Piperazine derivatives | Conv. of **2**[b] (%) | % of **1**[b] (%) | % of **4**[b] (%) |
|---|---|---|---|---|
| 1 | | 100 | 7.9 | 85.4 |
| 2 | | 100 | 3.9 | 86.3 |
| 3 | | 100 | 4.7 | 88.4 |

[a] Standard reaction conditions: substrate **2** = 20 mg (0.05 mmol) dissolved in 2 mL toluene/EtOAc = 1 : 1; 2 equivalents of piperazine derivative; $P_{sys}$ = 3 bar; $T$ = 90 °C; flow of reagents = 0.7 mL min$^{-1}$; flow of H$_2$ = 18 mL min$^{-1}$. [b] % determined by UHPLC; for details, see ESI.
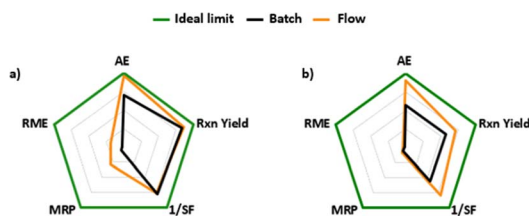


**Fig. 7** Comparison of green metrics between the batch and flow process of the reductive amination step (a) and the summary of the last two steps in the synthesis of CPL302415—oxidation and reductive amination (b).

performed jointly for the two steps of CPL302415 synthesis also showed the advantages of the flow process. For AE, rxn yield and SF (stoichiometric factor) metrics, we noted the values closer to

ideal for the flow procedure, while the MRP and RME remained almost identical for batch and flow transformations (Fig. 7b). However, the flow process demonstrates better green metrics: the most important is the high improvement of the total reaction yield from 57.8% to 71.6% when going from the batch to the flow process. Also, by conducting the reaction in the flow process, we managed to eliminate the DCM applied in batch reductive amination, which is considered as an undesirable solvent, and replaced it with the more favorable mixture of toluene and ethyl acetate.

Fig. 8 represents the overall E-factor profile. The diagrams (a) and (b) refer only to reductive amination step in the batch and flow process, respectively, while diagrams (c) and (d) show the E-factor profile jointly for oxidation and reductive

**Table 4** Comparison of the green metrics between the batch and flow process of the reductive amination step and summary of the last two steps in the synthesis of CPL302415—oxidation and reductive amination[a]

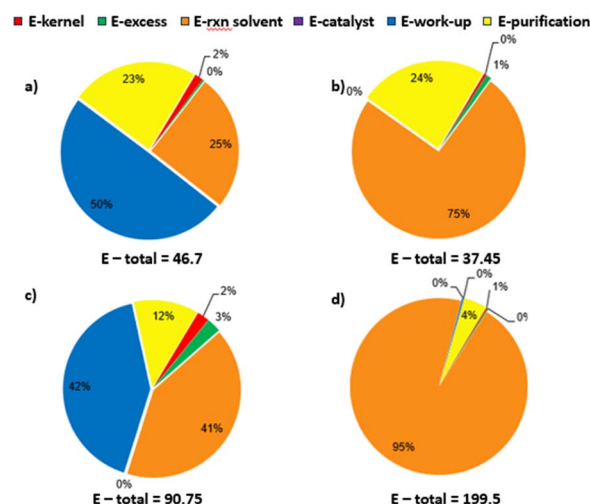| Green metrics | Batch | Flow | Ideal |
|---|---|---|---|
| **Reductive amination step** | | | |
| E-total | 46.7 | 37.7 | 0 |
| E-factor after solvent recycling | 37.2 | 4.3 | 0 |
| Yield | 83 | 86.4 | 100 |
| AE | 69.7 | 96.7 | 100 |
| PMI | 37.9 | 5.3 | 1 |
| RME | 2.6 | 18.9 | 100 |
| | | | |
| **Summary of oxidation and reductive amination steps** | | | |
| E-factor | 90.7 | 199.4 | 0 |
| E-factor after solvent recycling | 80.9 | 21.4 | 0 |
| Yield | 57.8 | 71.6 | 100 |
| AE | 56.4 | 90.7 | 100 |
| PMI | 81.9 | 22.4 | 1 |
| RME | 1.2 | 4.5 | 100 |

[a] For details, see ESI.



**Fig. 8** Comparison of the E-factor profile between reductive amination in batch (a) and in flow (b), and the summary of oxidation and reductive amination in batch (c), and telescoped oxidation and reductive amination in flow (d).

amination for batch and telescoped flow sequence, respectively. Both catalytic oxidation and especially reductive amination, which is carried out in the presence of a fixed-bed catalyst encapsulated in the metal cartridge and $H_2$ as the reductor, do not require such heavy workup like in the case of batch synthesis using $NaBH(OAc)_3$. Consequently, in flow reactions, the greatest impact on the E-factor profile is due to the solvents necessary to dissolve the substrates. These solvents can be easily recovered and recycled. Thus, the telescoped flow synthesis has initially a very high E-factor that reaches almost 200; it can be significantly improved up to 21.4 after solvent recycling (Table 4).

## Conclusions

We developed the interrupted telescoped flow sequence of oxidation and reductive amination as the key step in the synthesis of our new PI3Kδ inhibitor, CPL302415. The new flow sequence let us not only reach a higher yield of the desired product (increase from 57.8 to 71.6%) but we also achieved better green metrics in comparison to the batch synthesis. The above protocol was also generalized for the synthesis of other biologically active new PI3Kδ inhibitors based on the pyrazolo[1,5-a]pyrimidine core and applied to the quick building of the chemical library.

## Abbreviations

| AE | Atom economy |
|---|---|
| DMA | N,N-Dimethylacetamide |
| DoE | Design of experiment |
| E-factor | Environmental factor |
| E-rxn solvent | E-factor of solvents taken to dissolve the substrates |
| Eq. | Equivalents |
| MPR | Material recovery parameter |
| PMI | Process mass intensity |
| RME | Reaction mass efficiency |
| Rxn yield | Reaction yield |
| SF | Stoichiometric factor |

## Data availability

The authors confirm that the data supporting this study are included within the article and/or its ESI.†

## Author contributions

Synthesis, S. M., A. M.; analytical evaluation L. G.-B., W. M.; investigation, S. M., A. M.; reductive amination batch synthesis M. S.; writing-original draft preparation, S. M., A. M.; writing-review and editing, L. G.-B., W. M., K. W., M. Z.; DoE and statistical analysis: L. G.-B.; visualization A. M., and L. G.-B. All authors have read and agreed to the published version of the manuscript.

## Conflicts of interest

The authors declare the following financial interest/personal relationships which may be considered as potential competing interests. All contributors to this work at the time of their direct involvement in the project were full-time employees of Celon Pharma S.A. M. Wieczorek is the CEO of Celon Pharma S.A. Some of the authors are the shareholders of Celon Pharma S.A.

## Acknowledgements

## Notes and references

1 (a) P. Bianchi, A. Dubart, M. Moors, D. Cornut, G. Duhirwe, J. A. Vilanovac and J.-Ch. M. Monbaliu, *React. Chem. Eng.*, 2023, **8**, 1565; (b) N. S. Suveges, R. O. M. A. de Souza, B. Gutmann and C. O. Kappe, *Eur. J. Org Chem.*, 2017, 6511; (c) V. R. L. J. Bloemendal, M. A. C. H. Janssen, J. C. M. van Hest and F. P. J. T. Rutjes, *React. Chem. Eng.*, 2020, **5**, 1186; (d) P. Filipponi, B. Cerra, A. Piccinno, E. Camaioni and A. Gioiello, *Org. Process Res. Dev.*, 2024, **28**, 5–1648; (e) P. Bana, Á. Szigetvári, J. Kóti, J. Éles and I. Greiner, *React. Chem. Eng.*, 2019, **4**, 652; (f) M. Baumann and I. R. Baxendale, *Beilstein J. Org. Chem.*, 2015, **11**, 1194; (g) A. R. Bogdan and A. W. Dombrowski, *J. Med. Chem.*, 2019, **62**, 6422; (h) R. Porta, M. Benaglia and A. Puglisi, *Org. Process Res. Dev.*, 2016, **20**, 2; (i) F. M. Akwi and P. Watts, *Chem. Commun.*, 2018, **54**, 13894; (j) Z. Fülöp, P. Szemesi, P. Bana, J. Éles and I. Greiner, *React. Chem. Eng.*, 2020, **5**, 1527; (k) D. E. Fitzpatrick, C. Battilocchio and S. V. Ley, *ACS Cent. Sci.*, 2016, **2**, 131; (l) L. Malet-Sanz and F. Susanne, *J. Med. Chem.*, 2012, **55**, 4062; (m) R. Mougeot, P. Jubault, J. Legros and T. Poisson, *Molecules*, 2021, **26**, 7183; (n) A. S. Burange, S. M. Osman and R. Luque, *iScience*, 2022, **25**, 103892.

2 (a) M. C. F. C. B. Damião, R. Galaverna, A. P. Kozikowski, J. Eubanks and J. C. Pastre, *React. Chem. Eng.*, 2017, **2**, 896; (b) S. B. Ötvös, P. Llanes, M. A. Pericàs and C. O. Kappe, *Org. Lett.*, 2020, **22**, 8122; (c) A. D. Clayton, E. O. Pyzer-Knapp, M. Purdie, M. F. Jones, A. Barthelme, J. Pavey, N. Kapur, T. W. Chamberlain, A. J. Blacker and R. A. Bourne, *Angew. Chem., Int. Ed.*, 2023, **62**, e202214511; (d) F. Herbrik, M. Sanz, A. Puglisi, S. Rossi and M. Benaglia, *Chem.–Eur. J.*, 2022, **28**, e2022001; (e) G. M. Martins, M. F. A. Magalhães, T. J. Brocksom,

V. S. Bagnato and K. T. de Oliveira, *J. Flow Chem.*, 2022, **12**, 371; (f) M. di Filippo and M. Baumann, *Molecules*, 2021, **26**, 6992; (g) A. Steiner, R. C. Nelson, D. Dallinger and C. O. Kappe, *Org. Process Res. Dev.*, 2022, **26**, 2532; (h) P. S. Grant, M. A. Brimble and D. P. Furker, *Chem.–Asian J.*, 2019, **14**, 1128; (i) J. Jiao, W. Nie, T. Yu, F. Yang, Q. Zhang, F. Aihemaiti, T. Yang, X. Liu, J. Wang and P. Li, *Chem.–Eur. J.*, 2020, **27**, 4817.

3 (a) C. Jimenez-Gonzalez, A. D. Curzons, D. J. C. Constable and V. L. Cunningham, *Int. J. Life Cycle Assess.*, 2004, **9**, 115; (b) A. D. Curzons, C. Jimenez-Gonzalez, A. L. Duncan, D. J. C. Constable and V. L. Cunningham, *Int. J. Life Cycle Assess.*, 2007, **12**, 272.

4 L. Rogers and K. F. Jensen, *Green Chem.*, 2019, **21**, 3481.

5 (a) P. Bana, R. Örkényi, K. Lövei, Á. Lakó, G. I. Túrós, J. Éles, F. Faigl and I. Greiner, *Bioorg. Med. Chem.*, 2017, **25**, 6180; (b) Z. Brennan, https://www.in-pharmatechnologist.com/Processing/FDA-calls-on-manufacturers-to-begin-switch-from-batch-to-continuousproduction, accessed November 15th 2023.

6 (a) S. Michałek, L. Gurba-Bryśkiewicz, W. Maruszak, M. Zagozda, A. M. Maj, Z. Ochal, K. Dubiel and M. Wieczorek, *RSC Adv.*, 2022, **12**, 33605; (b) S. Michałek, A. M. Maj, L. Gurba-Bryśkiewicz, W. Maruszak, M. Zagozda, Z. Ochal, K. Dubiel and M. Wieczorek, *React. Chem. Eng.*, 2023, **8**, 1117; (c) S. Michałek, A. Powała, L. Gurba-Bryśkiewicz, *et al.*, *Monatsh. Chem.*, 2023, **154**, 1307.

7 M. Stypik, S. Michałek, N. Orłowska, M. Zagozda, M. Dziachan, M. Banach, P. Turowski, P. Gunerka, D. Zdżalik-Bielecka, A. Stańczak, U. Kędzierska, K. Mulewski, D. Smuga, W. Maruszak, L. Gurba-Bryśkiewicz, A. Leniak, W. Pietruś, Z. Ochal, M. Mach, B. Zygmunt, J. Pieczykolan, K. Dubiel and M. Wieczorek, *Pharmaceuticals*, 2022, **15**, 927.

8 (a) T. Saurat, F. Buron, N. Rodrigues, M.-L. de Tauzia, L. Colliandre, S. Bourg, P. Bonnet, G. Guillaumet, M. Akssira, A. Corlu, C. Guillouzo, P. Berthier, P. Rio, M.-L. Jourdan, H. Bénédetti and S. Routier, *J. Med. Chem.*, 2014, **57**, 613; (b) P. J. Parker, *Biochem. Soc. Trans.*, 2004, **32**, 893; (c) J. A. Engelman, J. Luo and L. C. Cantley, *Nat.*

*Rev. Genet.*, 2006, **7**, 606; (d) J. G. Foster, M. D. Blunt, E. Carter and S. G. Ward, *Pharmacol. Rev.*, 2012, **64**, 1027; (e) B. S. Safina, S. Baker, M. Baumgardner, P. M. Blaney, B. K. Chan, Y.-H. Chen, M. W. Cartwright, G. Castanedo, C. Chabot, A. J. Cheguillaume, P. Goldsmith, D. M. Goldstein, B. Goyal, T. Hancox, R. K. Handa, P. S. Iyer, J. Kaur, R. Kondru, J. R. Kenny, S. L. Krintel, J. Li, J. Lesnick, M. C. Lucas, C. Lewis, S. Mukadam, J. Murray, A. J. Nadin, J. Nonomiya, F. Padilla, W. S. Palmer, J. Pang, N. Pegg, S. Price, K. Reif, L. Salphati, P. A. Savy, E. M. Seward, S. Shuttleworth, S. Sohal, Z. K. Sweeney, S. Tay, P. Tivitmahaisoon, B. Waszkowycz, B. Wei, Q. Yue, C. Zhang and D. P. Sutherlin, *J. Med. Chem.*, 2012, **55**, 5887.

9 N. Shankaraiah, R. A. Pilli and L. S. Santo, *Tetrahedron Lett.*, 2008, **49**, 5098.

10 A. F. Abdel-Magid, K. G. Carson, B. D. Harris, C. A. Maryanoff and R. D. Shah, *J. Org. Chem.*, 1996, **61**, 3849.

11 C. G. F. Cooper, E. R. Lee, R. A. Silva, A. J. Bourque, S. Clark, S. Katti and V. Novorozhkin, *Org. Process Res. Dev.*, 2012, **16**, 1090.

12 A. E. Fitzgerald and N. S. Mani, *Synthesis*, 2012, **44**, 2469.

13 (a) S. A. May, M. D. Johnson, J. Y. Buser, A. N. Campbell, S. A. Frank, B. D. Haeberle, P. C. Hoffman, G. R. Lambertus, A. D. McFarland, E. D. Moher and T. D. White, *Org. Process Res. Dev.*, 2016, **20**, 1870; (b) M. D. Johnson, S. A. May, B. Haeberle, G. R. Lambertus, S. R. Pulley and J. R. Stout, *Org. Process Res. Dev.*, 2016, **20**, 1305.

14 (a) TIBCO Software Inc., *Data Science Textbook*, 2020, https://docs.tibco.com/data-science/textbook, accessed 15th November 2023; (b) *StatSoft's Electronic Statistics Textbook*, StatSoft Inc., 2006, https://www.statsoft.pl/textbook/stathome.html, accessed 15th November 2023.

15 (a) C. R. McElroy, A. Constantinou, L. C. Jones, L. Summerton and J. H. Clark, *Green Chem.*, 2015, **17**, 3111; (b) D. J. C. Constable, A. D. Curzons and V. L. Cunningham, *Green Chem.*, 2002, **4**, 521; (c) R. A. Sheldon, *ACS Sustainable Chem. Eng.*, 2018, **6**, 32; (d) J. Andraos and A. Hent, *J. Chem. Educ.*, 2015, **92**(11), 1820.